Electronic Supplementary Material (ESI) for Physical Chemistry Chemical Physics.
This journal is © the Owner Societies 2018

Supplementary Information:

Ultra-broadband EPR spectroscopy in field and frequency domains

P. Neugebauer[a,b†], D. Bloos[a], R. Marx[a], P. Lutz[a], M. Kern[a], D. Aguilà[c,d], J. Vaverka[b,e], O. Laguta[a], C. Dietrich[a], R. Clérac[c,d] and J. van Slageren[a‡]

[a.] *Institute of Physical Chemistry, University of Stuttgart, Pfaffenwaldring 55, D-70569 Stuttgart, Germany.*
[b.] *Central European Institute of Technology, CEITEC BUT, Technická 3058/10, 61600, Brno, Czech Republic.*
[c.] *CNRS, CRPP, UPR 8641, F-33600 Pessac, France.*
[d.] *Univ. Bordeaux, CRPP, UPR 8641, F-33600 Pessac, France*
[e.] *Institute of Physical Engineering, Brno University of Technology, Technická 2, 61669, Brno, Czech Republic.*
† petr.neugebauer@ceitec.vutbr.cz
‡ slageren@ipc.uni-stuttgart.de

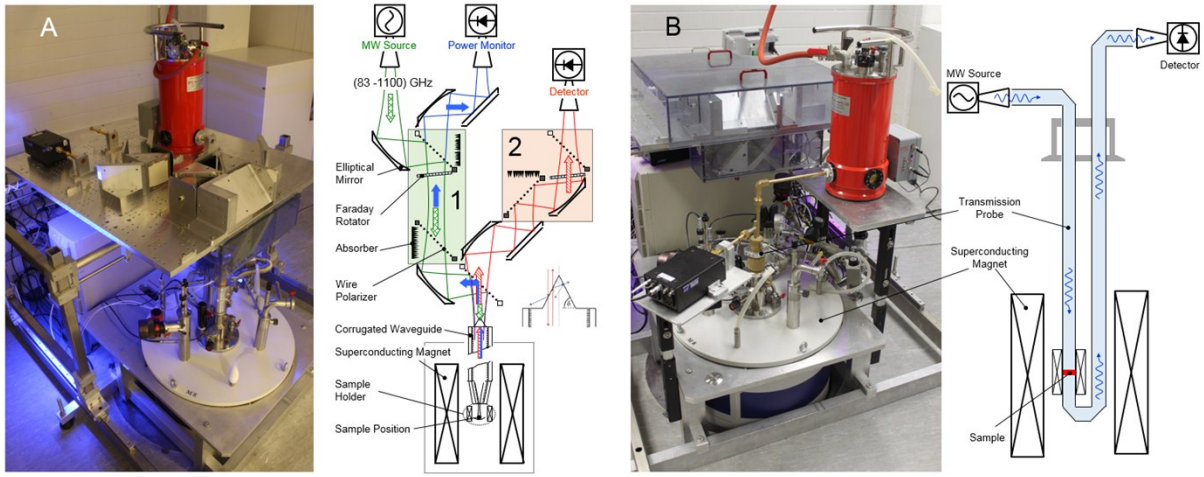

S1*: *Overall layout of the combined HFEPR/FDMR spectrometer in QO (A) and transmission (B) configuration.

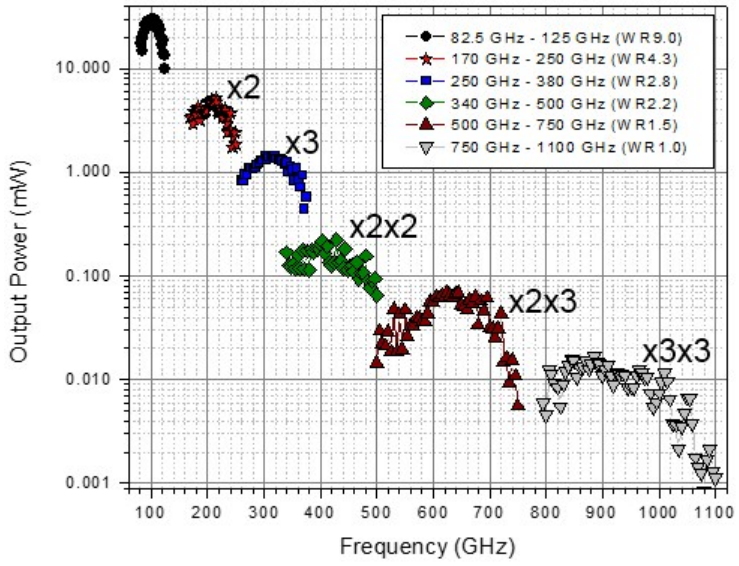

***S2:** Output power from the MW source based on Amplifier Multiplier Chain (AMC) and a series of full band frequency multipliers (THz Starter Kit Virginia Diodes Ltd.). At base frequency of 85-125 GHz the peak power is 37 mW (15,7 dBm) and it drops to about 0.01 mW (-20 dBm) after the highest frequency multiplication (9). The MW source output is in the 3 dB bandwidth in the 89% of the given multiplier output, only at the high frequency ends of the multiplier drops out of the 3 dB window.*

Sample Holders:

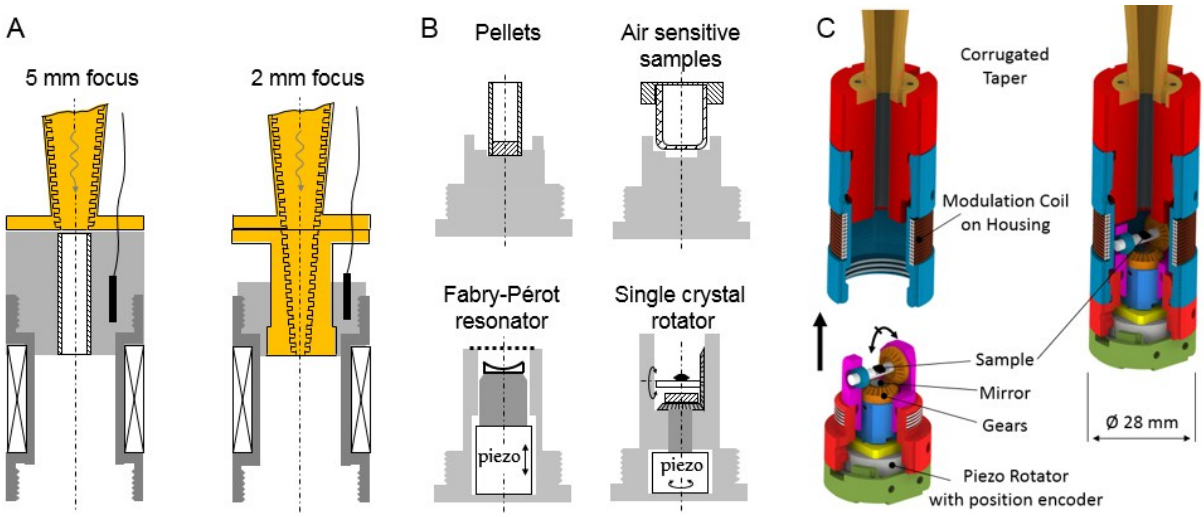

***S3**: Schematic view of the construction of available sample holders attached to our corrugated probe. A) Drawing of the different tapers with 5 mm or 2 mm focus. B) Drawings of the different sample holders: pellet sample holder, sample holder for air-sensitive samples, Fabry-Pérot resonator and single crystal rotator. C) Detailed 3D drawing of the single crystal rotator.*

The sample temperature is monitored by a Lakeshore CX-1050-AA calibrated Cernox temperature sensor. Mirrors used for reflecting the MWs back to the QO are gold coated. The Fabry-Pérot resonator in half-confocal configuration is formed by commercially available gold-coated concave mirrors of 12.7 mm in diameter and focal length of 50 mm (CM127-050-M01, Thorlabs Inc.). The planar mirror is home-made by UV-photolithography of golden inductive mesh on 18 mm in diameter and 200 µm thick fused silica cover slips (Gold-Seal). To tune the resonance in Fabry-Pérot resonator we use an Attocube ANPz51/LT linear piezo-stepper (range > 2.5 mm) with Attocube ANP300/ANM300 electronics with stepping/scanning module. The tuning is made by moving the bottom curved mirror with respect to static planar mirror. The performance of the Fabry-Pérot resonator was measured by N5225A PNA microwave network analyzer from Keysight Technologies with high frequency extenders from Virginia Diodes Inc., where we measured a Q-factor of 1200 at 330 GHz (S4).

In case of the single crystal rotator (S3C) we use an ANRv51/RES/LT piezo stepper with a resistive encoder providing information about the angle and the ANC350/3/RES/RT piezo motion controller.

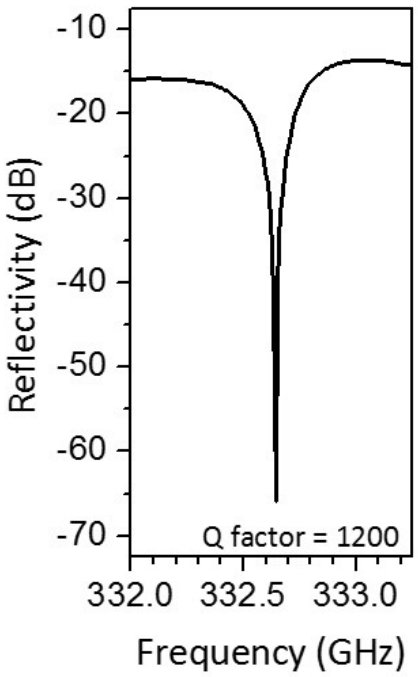

S4: *The performance of the Fabry-Pérot resonator was checked using N5225A PNA microwave network analyzer from Keysight Technologies with high frequency extenders from Virginia Diodes Inc. We measured a Q-factor of 1200 at 330 GHz, which is to our knowledge state of the art Fabry-Pérot resonator in HFEPR spectroscopy.*

Superconducting Magnet and Cryostat

For the generation of a strong magnetic field we use a superconducting solenoid (helium bath cryomagnet) with Variable Temperature Insert (VTI) from Oxford Instruments (INTEGRA system). The solenoid induces a magnetic field of 15 T and 17 T at 4.2 K and 2.2 K helium bath temperatures, respectively, where the cold bore is 52 mm. The maximal sweep rate of the magnet is 1 T/min in the entire range up to 15 T. The homogeneity of the magnetic field specified by the manufacturer is better than 100 ppm over a 10 mm sphere. By measuring the linewidth of Mn^{2+} in MgO at 380 GHz we obtained a homogeneity of about 10 ppm for a sample size of about 3 mm in diameter. The sample is located in VTI at temperatures in range of 1.8 K to 300 K with a sample space of 30 mm. To control temperature and magnetic field, MercuryiPS and MercuryiTC from Oxford Instruments are used. The Mercury system also monitors the amount of cryogenic liquids (N_2 and He). The entire magnet is about 1.8 m toll and 0.8 m in diameter. In order to have the quasi-optics in a comfortable height and to allow comfortable loading of the 1.8 m long corrugated waveguide into the cryostat, the magnet is fixed to the spectrometer frame by its top part by a rim and the main part of the magnet is under the laboratory floor (Figure S2B).

Microwave Detection

ST1: *Selected parameters of used MW detectors.*

Detector	Operation Frequency	NEP	Bandwidth	MW coupling
QMC Bolometer	60 GHz - 1.8 THz	1.5 pW/Hz$^{1/2}$ at 275 GHz	1 MHz	optical
VDI WR2.8 ZBD	(260 – 400) GHz	Typical 4.1 pW/Hz$^{1/2}$	approx. 40 GHz	waveguide
VDI WR4.3 ZBD	(170 – 260) GHz	Typical 3.5 pW/Hz$^{1/2}$	approx. 36 GHz	waveguide

Control Software

To control the HFEPR/FDMR spectrometer we use GPIB (lock-in amplifier) and ethernet (magnet, temperature controller) interfaces of the used electronic devices and -home-written control program in LabVIEW (G-Code). The software offers an easy and straightforward graphical user interface for control of the main parameters of the spectrometer, e. g., frequency, magnetic field, temperature and in case of single crystal rotator also the orientation of a sample. We have implemented a script-based automation of the measurements. The parameters controlled from the script are: MW frequency (in a range of selected a broadband multiplier), magnetic field range (-15 T – 15 T), sweep rate (T/min or MHz/s in case of EPR and FDMR, respectively), temperature (1.8 K – 300 K), waiting time (in minutes) and set angle (0° - 340°). Measurement parameters and spectrometer settings are automatically saved in the measurement files. During a measurement the software permanently monitors the key parameters of the spectrometer, such as the status of cryogenics liquids and even electric power interruption. In case of a hazardous situation, for example a low level of cryogenic liquids or blackout, an emergency shutdown is implemented, which will bring the HFEPR/FDMR spectrometer to a safe state using an uninterruptable power supply (UPS) and informs the user about the shutdown via E-Mail. Thanks to the high level of safety implemented, unattended measurements are commonly performed, leading to efficient use of the spectrometer time by performing experiments from script at nights and weekends.

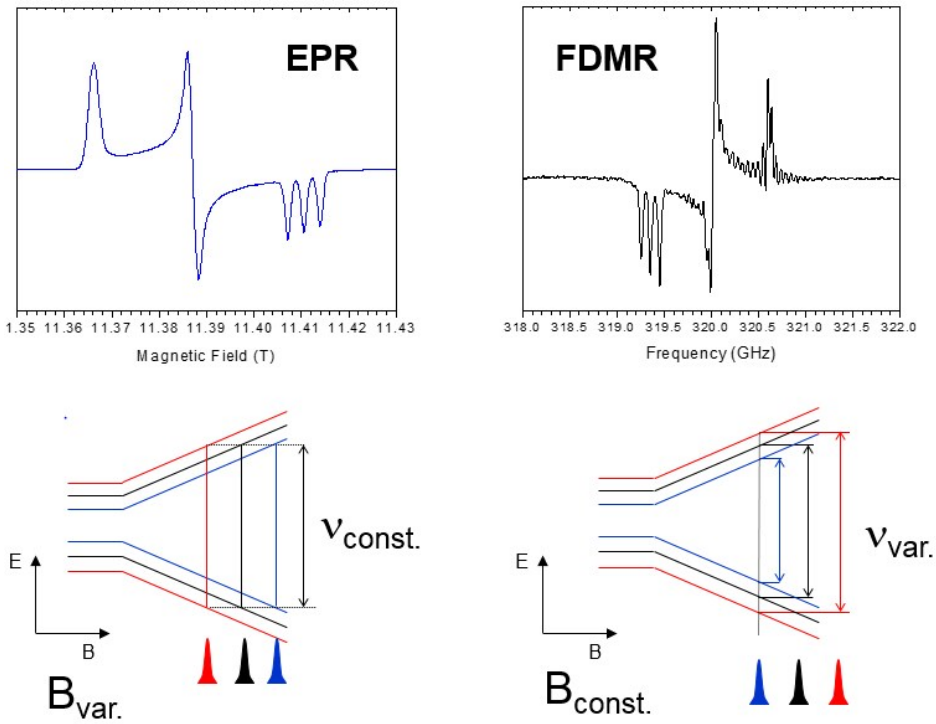

S5: *Explanation of appearance of EPR and FDMR spectra. While in EPR the MW frequency is kept constant and the spectrum is recorded as a function of magnetic field, in FDMR it is opposite. This results in an "inverted" spectrum. In EPR the first observed transition is that which corresponds to the highest g-value whereas in FDMR it is the last, as is shown is the figures below.*

Sensitivity determination:

The EPR spectrometer sensitivity which can be expressed by the minimum detectable number of spins $Nmin$ is proportional to a number of terms[1]:

$$N_{min} \propto \frac{VsTs}{\eta Q}\left(\frac{\Delta fpp}{fex}\right)\left(\frac{\Delta Bpp}{Bmod}\right)\left(\frac{FT_d\Delta f}{P0}\right)^{1/2} \qquad (1)$$

ST2: *EPR spectrometer depending parameters of above equation.*

symbol	*meaning*
Vs	Sample volume
Vc	Cavity volume
Ts	Sample temperature
η	Filling factor, $\eta \approx Vs/Vc$
Q	Quality factor
Δfpp	*Peak to peak linewidth*
fex	*Excitation frequency*
ΔBpp	Peak to peak linewidth, $\Delta fpp = \gamma e \Delta Bpp$
$Bmod$	Modulation field amplitude
F	Noise figure
T_d	Detector temperature
Δf	Detection bandwidth
$P0$	Incident microwave power

From equation (1) it is clear that a large irradiation power $P0$, a high quality factor Q and a high applied field B (thus frequency) leads to higher sensitivity, meaning a lower number of spins $Nmin$.

However as many of the parameters are in our case not well determined, the spectrometer's absolute sensitivity was determined from a concentration dependence of the SNR (varying the number of spins, compare S6) of BDPA (from Sigma Aldrich). The slope of such a dependence determines the number of spins that corresponds to SNR = 1. Using this approach, we obtained $(4.40 \pm 0.08) \times 10^{11}$ spins, and if we divide it by the linewidth (17 G) and our detection bandwidth (3 Hz) this will lead to the sensitivity of $\approx 10^{10} Spins/G\sqrt{Hz}$ at $fex = 370\ GHz$ and $Ts = 60\ K$ using our pellet insert (S3B).

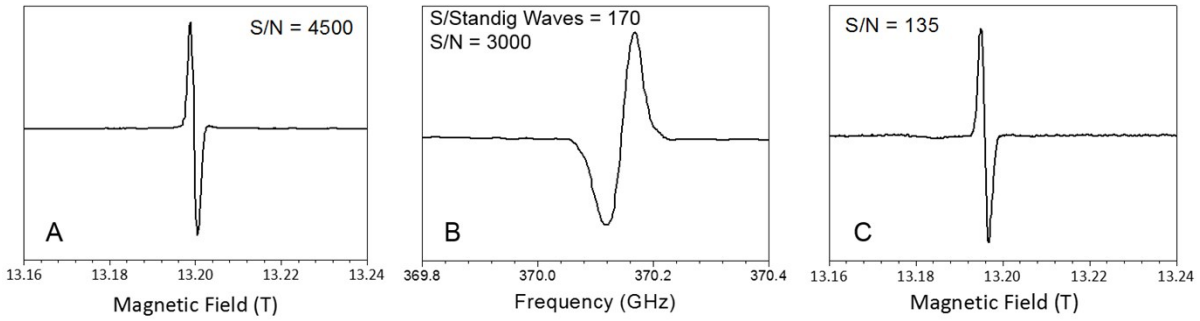

S6: *A) HFEPR spectrum of a 1 µM BDPA in a PS film at 60 K, at 370 GHz and at 15 G modulation amplitude, 1 kHz modulation frequency and 300 ms time constant. The sample contained 2.0·10[15] spins, B) FDMR spectrum of the same sample at 13.2 T, with a sweeping rate of 25 MHz/minute and at the same modulation condition as in A. C) HFEPR spectrum of a 0.1 µM BDPA in PS film at 60 K, at 370 GHz and at 15 G modulation amplitude. The sample contained approximately 1.0·10[14] spins.*

For other sample temperatures the minimum number of spins can be estimated by calculating the Boltzmann factor α:

$$\alpha = e^{-\frac{\Delta E}{kBTs}}$$

where $\Delta E = g\mu BB = 2.45 \cdot 10^{-22} J$ and kB is the Boltzmann constant. For $Ts = 5\ K$ this leads to a value $\alpha(5\ K) = 2.88 \cdot 10^{-2}$, $\alpha(60\ K) = 7.44 \cdot 10^{-1}$ for $Ts = 60\ K$ and $\alpha(300\ K) = 9.43 \cdot 10^{-1}$ for $Ts = 300\ K$.

Now, N_{min} for $Ts = 5\ K$ can be estimated in the following way:

$$N_{min}(5\ K) \approx\ N_{min}(60\ K) \cdot \left(\frac{a_{5K}}{a_{60K}}\right) \approx\ 3.8 \cdot 10^{8} spins/(G\sqrt{Hz})$$

$$N_{min}(300\ K) \approx\ N_{min}(60\ K) \cdot \left(\frac{a_{300K}}{a_{60K}}\right) \approx\ 1.3 \cdot 10^{10} spins/(G\sqrt{Hz})$$

In the case of the Fabry-Pérot-Resonator, it is one order of magnitude better (Figure 2.) leading to overall estimated of absolute sensitivity at the order of **10^7 spins/(G.Hz$^{1/2}$)** and **10^9 spins/(G.Hz$^{1/2}$)** at 5 K and 300 K at 370 GHz, respectively. Note that this estimation is not taking in to account change of relaxation times with temperature.

The concentration sensitivity, which is often of interest concerning biological samples, can be obtained by dividing $Nmin$ by the sample volume $Vsample$. For our particular measurement the concentration sensitivity at $Ts = 60\ K$ can be estimated for a sample volume of $Vsample = 0.01\ cm^3$:

$$Nmin/Vsample \approx 10^{12}\ spins/G \cdot cm^3\sqrt{Hz}$$

and can be further improved by enlarging the sample volume in some extend.

Due to the good sensitivity, we were furthermore able to perform for the first time FDMR measurements on small single crystals (e. g. 0.1 mg of $Mn_{12}Ac$) (S7). Single crystal FDMR experiments on small crystals were in the past very difficult or almost impossible because the FDMR experiments were performed as a single pass transmission and the obtained signal was dominated by standing waves.

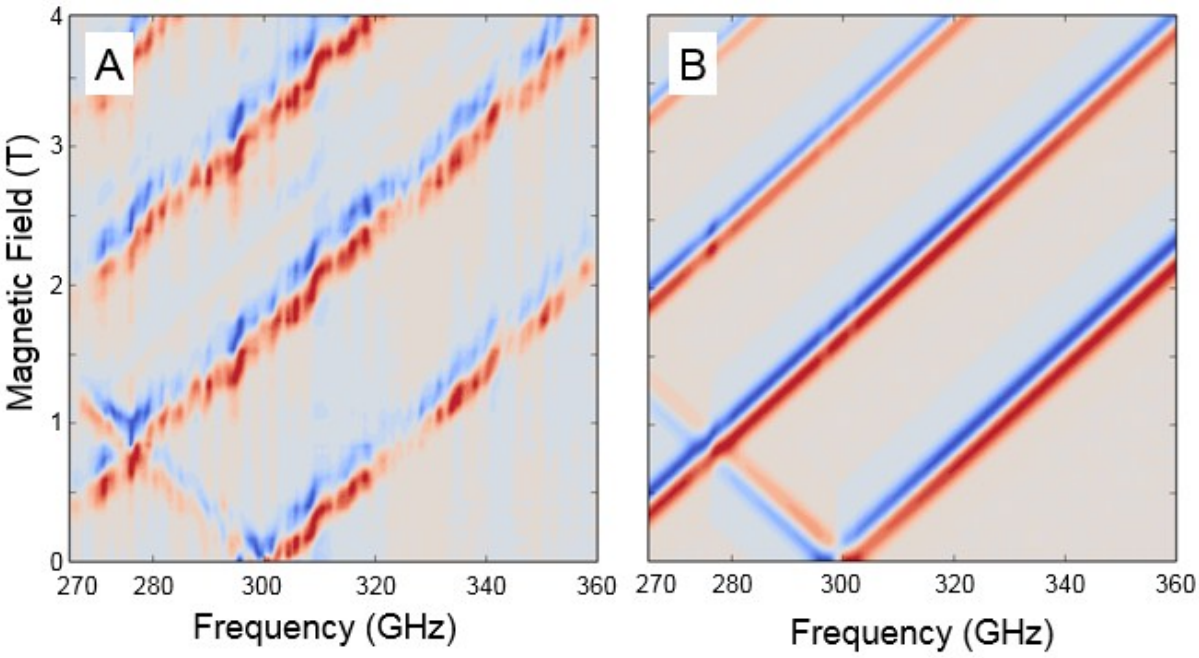

S7: *(A) FDMR map of a needle shaped, single crystal of $Mn_{12}Ac$ of a size approximately 1 mm x 0.3 mm x 0.3 mm and mass about 0.1 mg, recorded at 30 K and several magnetic fields. The FDMR map was created by 160 FDMR scans, where each took about 10 seconds. (B) Corresponding Easyspin[2] simulation.*

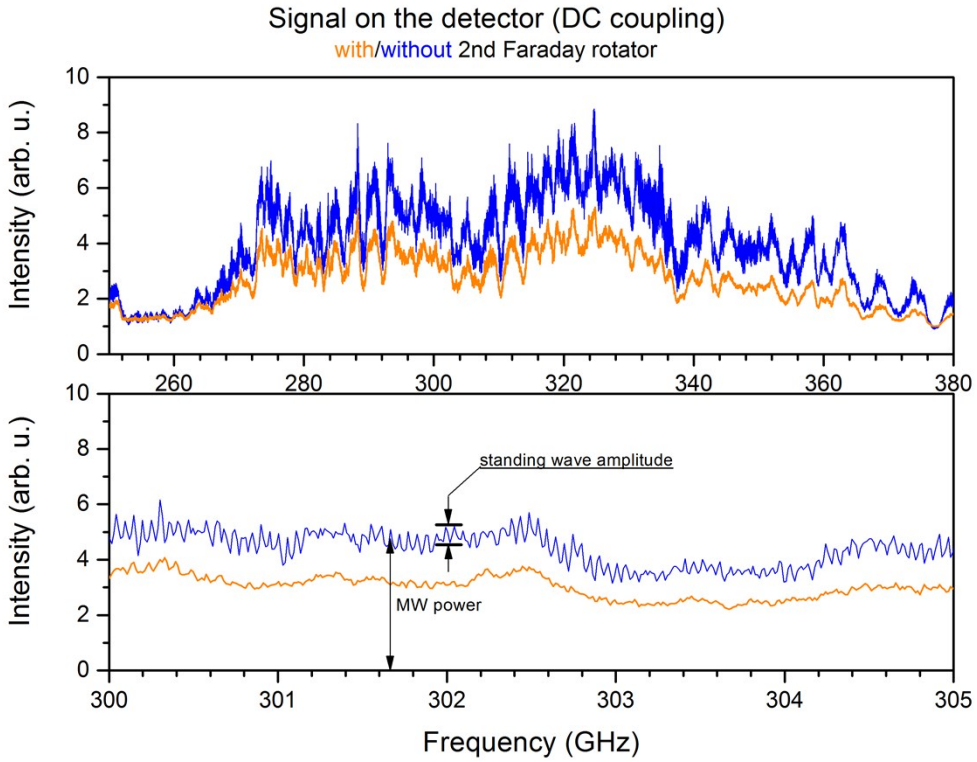

***S8**: To the explanation on the standing wave amplitude.*

For quantitative comparison of the standing waves' amplitude A_{sw} with respect to the microwave power P_{MW}, we recorded direct signal (no modulation) on the detector as a function of microwave frequency. Figure S13 shows an example of such a spectrum in 250-380 GHz range. The standing waves can be easily seen in the magnified spectrum. The relative amplitude of a standing wave can be estimated as

$$A_{rel} = \frac{A_{sw}}{P_{MW}}$$

It should be emphasized that the introduction of the second Faraday rotator (See Figure S1A. Pos. 2) markedly decreases standing waves, namely from $A_{rel} \approx 0.2$ to $A_{rel} \approx 0.075$.

Mn2 single chain complexes:

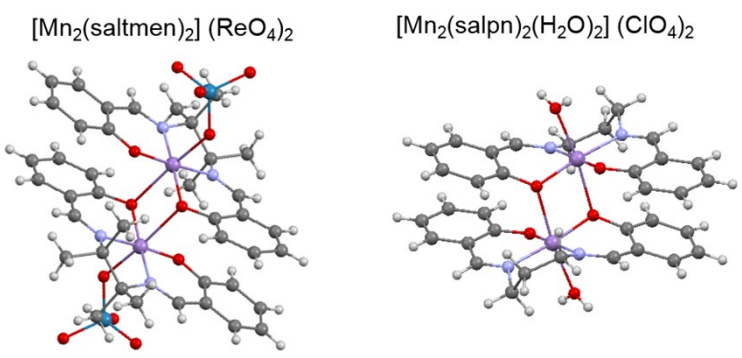

***S8:** Molecular structure of Mn_2 complexes.*

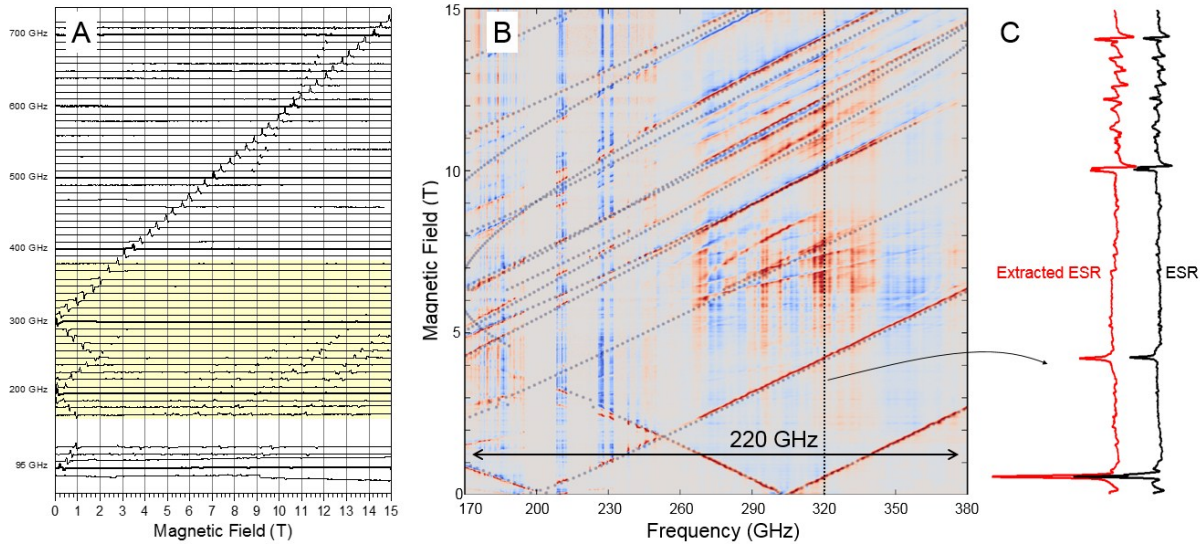

S9: *HFEPR measurement of complex **1** at 30 K and frequencies up to 720 GHz (A), frequencies within the yellow area were used for the high resolution 220 GHz wide FDMR map(B). The map with 10000 points x 20000 points in magnetic field and frequency direction, respectively, was recorded in only 8 hours of measurement time. Comparison of HFEPR spectra extracted from the map at 320 GHz and the conventionally recorded HFEPR at the same frequency (C).*

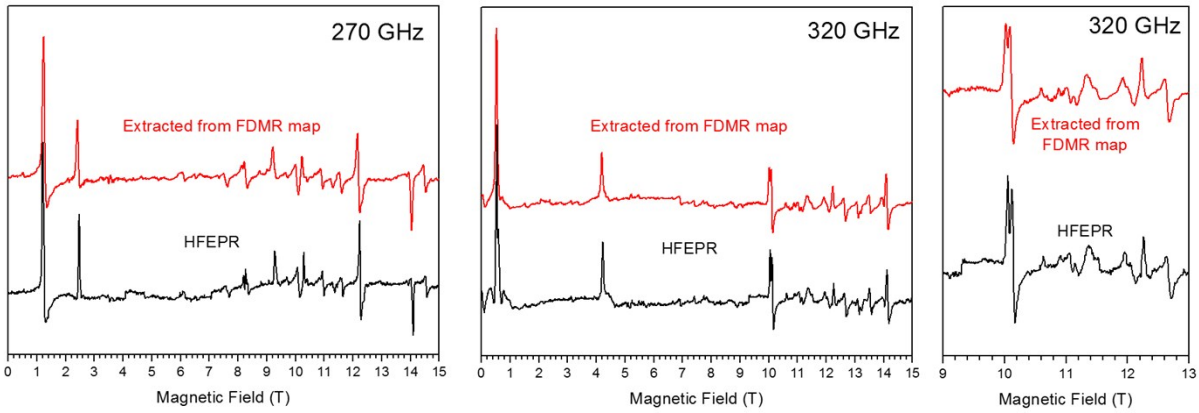

S10: *Comparison of HFEPR measurement and extracted HFEPR from the high resolution map on S9.*

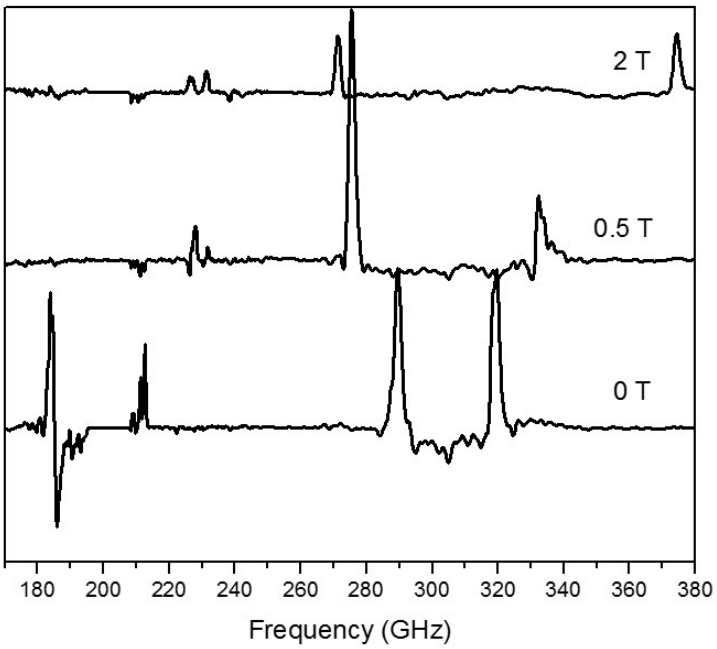

S11: *FDMR spectra extracted from Fig10B at 0, 0.5 and 2 T.*

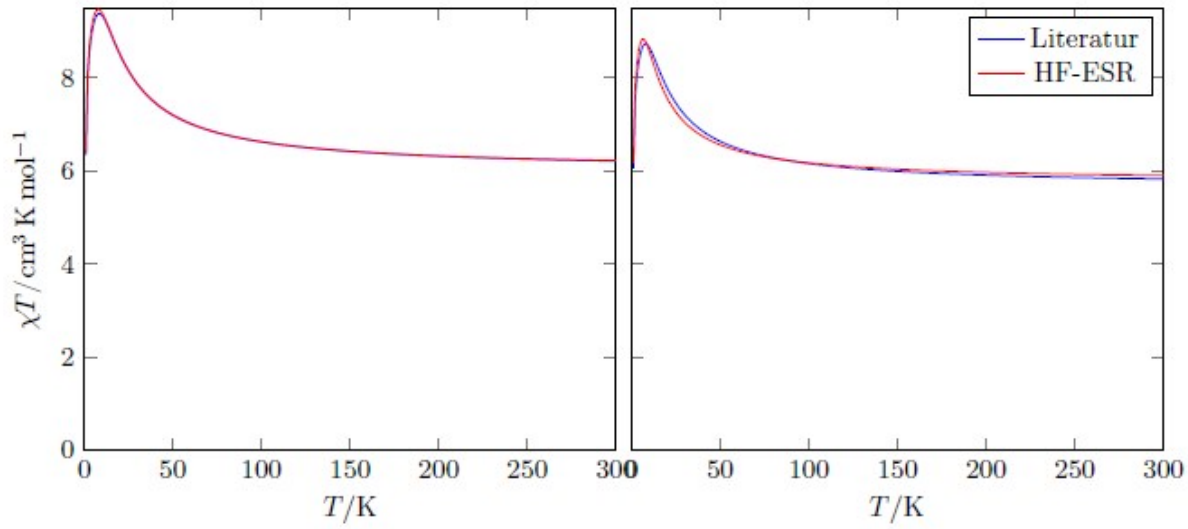

S12: *Calculated susceptibility of Mn_2saltmen (left) and Mn_2salpn (right) using parameters listed in Table 1.*

REFERENCES:

1. C. P. Pool, *ELECTRON SPIN RESONANCE: A Comprehensive Treatise on Experimental Techniques.*, Dover Publications, Mineola, New York, second edn., 1997.
2. S. Stoll and A. Schweiger, *J. Magn. Reson.*, 2006, **178**, 42-55.